Acta Geodyn. Geomater., Vol. 22, No. 3 (219), 381–392, 2025
DOI: 10.13168/AGG.2025.0026
journal homepage: https://www.irsm.cas.cz/acta

ORIGINAL PAPER

THE INTERPRETATION OF EIGEN-6C4 SATELLITE GRAVITY DATA DETECTS THE MAJOR STRUCTURAL FAULTS AND BASEMENT DEPTH IN THE SOUTHERN PART OF JABAL NAFUSAH, NORTHWESTERN LIBYA

Fouzie TREPIL[1, 2], Nordiana Mohd MUZTAZA [1, 4] *, Ismail Ahmad ABIR [1], Mohamed A. SALEEM [3] and Khiri Abubaker KHAlf [1]

[1] *School of Physics, Universiti Sains Malaysia 11800, Pulau Penang, Malaysia*
[2] *Geophysics Dept., Faculty of Science, University of Tripoli, PO Box 13275, Tripoli, Libya*
[3] *Petroleum Institute (LPI), Tripoli, 6431, Libya*
[4] *Centre of Tropical Geoengineering (GEOTROPIK), Universiti Teknologi Malaysia, D03, Faculty of Civil Engineering, 81310 Skudai, Johor, Malaysia*

**Corresponding author's e-mail:* mmnordiana@usm.my

ARTICLE INFO

Article history:
Received 29 April 2025
Accepted 12 August 2025
Available online 24 August 2025

Keywords:
Major Faults
Basement depth
EIGEN-6C4 gravity
Jabal Nafusah
Libya

ABSTRACT

Despite the long history of petroleum exploration in Libya—spanning over 55 years—limited research has been conducted on the tectonic evolution of its southern margin within the central Mediterranean Basin. The structural framework of this region remains poorly understood, necessitating further investigation. This study utilises EIGEN-6C4 satellite gravity data from the southern region of Jabal Nafusah in northwestern Libya to identify key subsurface structures and estimate basement depths. The gravity data were analysed and converted into a geophysical model using the Oasis Montaj software to achieve these objectives. Several analytical techniques were applied, including high-pass filtering, tilt derivative (TDR), total horizontal gradient (THG), and Euler deconvolution (ED), to enhance the interpretation of subsurface features. Additionally, 2D forward modelling using the GM-SYS tool within Oasis Montaj was employed to determine the depths of gravity anomalies associated with the basement. The findings reveal fault systems with varying orientations, primarily NE-SW and NW-SE and source depths ranging from 1,200 m to 5,798 m, indicating a complex tectonic history. The integration of 3D Euler solutions with residual gravity anomalies provided more accurate locations and depth estimates for these subsurface structures. Basement depth analysis along different profiles showed variations, with Profile 1 ranging from 1.2 km to 3.53 km, Profile 2 from 1.8 km to 2.7 km, and Profile 3 from 1.7 km to 2.76 km. This study highlights the effectiveness of satellite gravity data in characterising geologically underexplored regions, offering valuable insights into the structural framework and potential resource prospects of northwestern Libya.

1. INTRODUCTION

Northwestern Libya is characterised by complex subsurface geological structures influenced by various tectonic events, including the Caledonian and Hercynian orogenies. However, the region's structural framework, fault systems, and basement depth variations remain insufficiently understood due to limited geophysical investigations. Identifying linear anomalies is crucial for detecting subsurface structures such as lithological contacts, faults, folds, and fractures, which helps in understanding potential field data (Miller and Singh, 1994; Ma and Li, 2012; Zhang et al., 2015). Studying lithological units, contacts, lineaments, faults, and dykes is a key aspect of structural analysis (Masoud and Koike, 2011; Salehi et al., 2015). Northwestern Libya is an integral part of the structurally complex eastern flank of the South Atlas Fold Belt, positioned adjacent to the Saharan Flexure or Lineament. This region exhibits intricate geological features shaped by tectonic interactions, contributing to its dynamic structural framework. Consequently, this research is highly significant in advancing the understanding of subsurface geological structures in northwestern Libya. The study provides a comprehensive analysis of regional tectonics, fault systems, and basement depth variations. The findings have substantial implications across multiple disciplines. The potential field method is commonly used to map the depth and extent of structural features in a region. Analysis of satellite gravity data plays a crucial role in the initial phases of exploration, offering an effective means of assessing geological conditions in large or remote areas (Kurniawan and Aji, 2012; Sadeghi et al., 2013; Zeinelabbdein et al., 2014). Gravity data can be utilised to define subsurface structures and estimate the depth of basement rocks, helping locate basins, which are ideal sites for oil accumulation (Araffa et al., 2015). The study area, located in the southern part of Jabal Nafusah, northwest Libya (between 12.10 and 12.80 degrees east and 31.50 and 31.80 degrees north), is of significant interest to various oil exploration companies. Several geological and geophysical studies have been conducted in northwest Libya, employing gravity, magnetic, and remote sensing data to investigate the surface and structures beneath the

Cite this article as: Trepil F, Muztaza NM, Abir IA, Saleem MA, Khalf KA: The interpretation of EIGEN-6C4 satellite gravity data detects the major structural faults and basement depth in the southern part of Jabal Nafusah, northwestern Libya. Acta Geodyn. Geomater., 22, No. 3 (219), 381–392, 2025. DOI: 10.13168/AGG.2025.0026

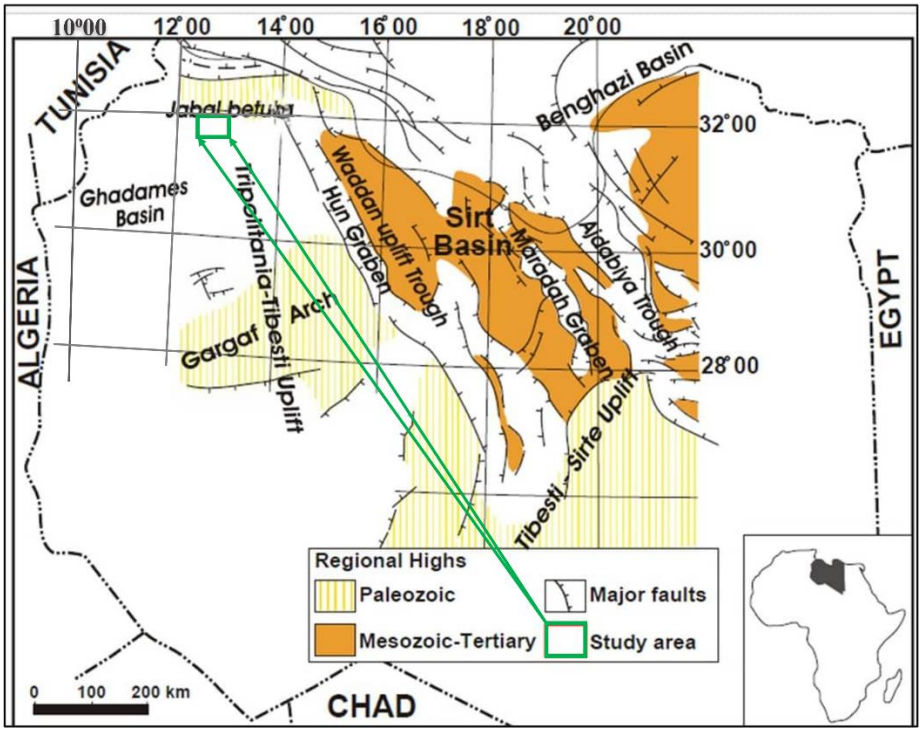

Fig. 1 Presentation both the geographic location of the study area, highlighted within a green rectangle, and a simplified geological map that provides an overview of the region's lithological and structural features. The geological map has been adapted and refined from the work of Rusk (2001) to enhance clarity and relevance to this study.

surface by Desio et al. (1963), Christie (1966), Steckler et al. (1988), Swire and Gashgesh (2000), Saadi et al. (2009, 2011) and Trepil et al. (2023, 2024). The boundaries of geological bodies are crucial for gravity data processing and interpretation, as they are often linked to prominent discontinuities, such as faults, unconformities, or intrusive contacts (Pal et al., 2016). This study employed several methods, including high-pass filtering, total horizontal gradient analysis, tilt derivative, Euler deconvolution, and basement depth estimation, to identify major structures in the area.

GEOLOGICAL SETTING

The study area (Fig. 1) is part of the North African Platform, characterised by NE-SW and NW-SE lineaments formed during the early Paleozoic era. This platform has experienced a complex and polyphase geological history, shaped by multiple tectonic events. The primary tectonic elements in the region underwent significant transformations starting from the Late Precambrian Pan-African orogeny, continuing through the Phanerozoic with repeated reactivation of older structures. The region is also considered part of the structurally intricate Atlas fold belt, formed by tectonic plate collisions followed by the folding and uplifting of the Earth's crust. The area's complex geological evolution can be summarised in three key stages: Hercynian Orogeny: The North African Platform underwent the Hercynian Orogeny, which created a large, subsiding depositional basin with minimal regional differentiation. This basin formed as the Pan-African fault system became active once more (Van de Weerd and Ware, 1994). During the Hercynian phase, the basin was uplifted and eroded, removing much of the Paleozoic strata across the region. Mesozoic Rifting: Following the Hercynian phase, northwest tilting occurred, resulting in the formation of a Mesozoic extensional basin over the eroded Paleozoic basin (Van de Weerd and Ware, 1994; Echikh, 1998). This phase was marked by a series of uplifts throughout the Phanerozoic, with basins in Northwest Africa intersecting diagonally, as noted by Klitzsch (1970) and Klitzsch and Gray (1971). He also proposed that the Caledonian tectonic period revived an earlier Pan-African suture zone, which became crucial to the formation of the east-west-orientated "Nafusah arch". The Nafusah Uplift, located in the northern part of the study area, initially uplifted during the Hercynian orogeny before subsequently undergoing subsidence. In the early Mesozoic, tectonic activity led to rifting in the southern section of the Nafusah Arc, a significant east-west-orientated structural feature that serves as a geological boundary between the Ghadames and Jifara basins (Abohajar et al., 2009). Lipparini (1968) attributed the northwest-southeast displacement observed in the region to the uplift process, while Mann (1975) suggested that the structural development of Jabal Nafusah effectively concluded by the late Cretaceous. The Ghadames Basin, which lies adjacent to the uplift, contains a stratigraphic

sequence spanning from the Paleozoic to the Cenozoic, reflecting a long and complex depositional history. Within the study area, the sedimentary succession consists predominantly of clastic carbonate formations, including sandstone, limestone, clay, and marl (Christie, 1955; Burollet, 1963; Mann, 1975). These rock units date from the Middle Jurassic to the Quaternary, indicating a prolonged period of sediment accumulation influenced by regional tectonic and paleoenvironmental conditions. The Pan-African orogeny, occurring in the Neoproterozoic, initiated the formation of the Al Hamra Basin, which was later reactivated during the subsidence of the Paleozoic basin (Echikh, 1998). The Al Hamra plateau, which is predominantly flat (Fig. 1), consists mostly of exposed Paleocene limestone, with late Cretaceous limestone forming its borders. Large Maastrichtian limestone surfaces cover the plateau along the north-northwest edge, likely due to southward dips and the slight elevation of the border near the Nafusah arch to the north. The weathering and erosion processes were likely more intense at higher elevations, leading to the removal of Paleocene sediments in those areas. The geological evolution and structural characteristics of the region have been profoundly shaped by a series of major tectonic events, including the Caledonian, Hercynian, and Alpine orogenies. These events played a crucial role in influencing sediment deposition patterns, leading to the accumulation of extensive continental clastic deposits and a dynamic history of marine transgressions and regressions. As a result, a diverse range of sedimentary rock formations developed over time, reflecting shifting environmental conditions and tectonic influences. Since the Precambrian era, the area has undergone multiple cycles of uplift and subsidence, accompanied by structural deformation processes such as folding and crustal consolidation. This long-term geological evolution began with the Pan-African Orogeny (Anketell, 1996), a significant tectonic event that contributed to the initial formation of the region's structural framework. Additionally, this period was marked by intense metamorphic activity, which facilitated the reworking and remobilisation of ancient cratonic margins, further shaping the region's deep-seated geological structures (Hallet, 2002).

2. MATERIALS AND METHOD

The EIGEN-6C4 gravity data used in this study were acquired from the "International Centre for Global Earth Models" (ICGEM) database. Satellite gravity data analysis serves as a valuable exploratory tool for identifying subsurface geological structures. This approach is based on detecting variations in the density distribution of underground materials, which result in corresponding changes in the Earth's gravitational field. By analysing these gravitational variations, researchers can delineate subsurface formations, estimate basement depths, and identify potential sedimentary basins that may be conducive to hydrocarbon accumulation (Araffa et al., 2015). The dataset comprises 2,304 gravity data points arranged in a grid with a spatial resolution of 0.01° x 0.01°. Numerous geological and geophysical studies have employed EIGEN-6C4 gravity data to investigate structural features in various regions (Tedla et al., 2011; Pal and Majumdar, 2015; Darisma et al., 2019; Trepil et al., 2024). Initially, the gravity data were collected as free-air anomalies. To enhance accuracy, the datasets were corrected by removing the gravitational influence of the rock mass between the measurement station and mean sea level, producing the Bouguer gravity anomaly. To further refine the analysis, the Bouguer gravity anomaly grid (Fig. 3) was generated using the least-curvature random gridding technique. Additionally, the EIGEN-6C4 gravity model was applied to derive a residual gravity anomaly map, analyse total horizontal gradient variations, compute tilt derivative values, conduct Euler deconvolution, and estimate basement depths across the study area. These advanced processing techniques provided a comprehensive understanding of the geological framework and structural composition of the region.

- **High-pass Filter**

Two types of Bouguer gravity anomalies exist: (i) regional gravity anomalies, which originate from a deep source, and (ii) residual gravity anomalies, which originate from the near surface. A regional anomaly is characterised by long wavelengths and low frequencies (Subba Rao, 1996). Residual anomalies are relatively characterised by short wavelengths and high frequencies (Subba Rao, 1996). The Gaussian high-pass filter has been used to separate residual gravity anomalies from regional anomalies. This filtering technique is designed to selectively allow or eliminate specific ranges of wavenumbers from the dataset. By applying this filter, certain frequency components associated with geological structures of interest can be enhanced, while unwanted noise or irrelevant features are suppressed. The residual anomaly equation (1) is obtained as

$$g_{reidual}(x,y) = g_{bouguer}(x,y) - g_{regional}(x,y) \quad (1)$$

- **Total Horizontal Gradient (THG)**

The THG equation (2), which utilises upright contacts, helps to identify the boundaries of gravity anomalies. It is expected that geological contacts in the study area will be more clearly visible after applying a horizontal gradient filter. The horizontal gradient method, introduced in 1982, has been used to delineate boundaries from gravity data (Cordell, 1979). This technique is based on the principle that a nearly vertical fault-like boundary produces a gravity signature, with the maximum horizontal gradient occurring at the edge of the boundary. In general, gravity anomaly derivatives highlight shallow structures, reduce the influence of regional anomalies, and eliminate the effects of deeper structures.

Table 1 Provides the structural index used for gravity anomaly interpretation, as described by FitzGerald et al. (2004).

Source	Gravity
Sphere	2
Horizontal	1
Fault	0

$$\mathrm{HG}(x,y) = \sqrt{\left(\frac{\partial G}{\partial x}\right)^2 + \left(\frac{\partial G}{\partial y}\right)^2} \quad (2)$$

The gravity anomaly, denoted as G, is a measure of the deviation from the expected gravitational field. The magnitude of the horizontal gradient at a given position (x, y) is denoted as HG (x, y). The calculation is based on the partial derivatives of the gravity anomaly with respect to the horizontal coordinates x and y, denoted as ∂G/∂x and ∂G/∂y. These derivatives represent the rate of change of the gravity anomaly along the x and y axes, respectively. By computing these partial derivatives, we can obtain the gradient of the gravity anomaly, which provides valuable information about the variations in the subsurface structure.

- **Tilt angle derivative (TDR)**

Miller and Singh (1994) developed the tilt angle derivative (TDR) as a technique for analysing gravitational anomalies. The TDR is calculated as the arctangent of the ratio between the vertical derivative and the combined horizontal derivatives of the gravity field, as shown in equation (3). This method helps to estimate the depth and location of subsurface anomalous sources, assuming these sources can be modelled as two-dimensional structures. The tilt angle derived from TDR can indicate the edges of these anomalies, providing key insights into the subsurface geology. The TDR, also referred to as the Total Derivative Ratio, is particularly effective in enhancing the visibility of gravitational anomalies by focusing on both the vertical and horizontal variations in the gravity field (Ming et al., 2021). This technique allows for a clearer distinction of the sources of gravitational anomalies, making it valuable in geophysical exploration and geological studies.

$$\mathrm{TDR} = \tan^{-1}\left\{\frac{\frac{\partial G}{\partial z}}{\sqrt{\left(\frac{\partial G}{\partial x}\right)^2 + \left(\frac{\partial G}{\partial y}\right)^2}}\right\} \quad (3)$$

The coordinates (x, y) denote the specific point in space where the gravity field, denoted as G, is measured. The terms (∂G/∂x) and (∂G/∂y) refer to the horizontal derivatives of the gravity field, which describe how the gravitational field changes with respect to variations in the horizontal direction, either along the x-axis or the y-axis. The symbol (G/z) represents the vertical derivative of the gravity field, which indicates how the gravity field changes with respect to vertical variations, or the z-axis.

- **Euler deconvolution**

The Euler solution method, as outlined in equation (4), provides an effective means of estimating both the depth and location of different homogeneous gravity sources. This method incorporates a structural index, which is an exponential variable that defines the characteristics of geological bodies, as detailed in Table 1. One of the key advantages of this approach is its ability to deliver reliable results with minimal prior knowledge about the source body's structure, making it particularly useful in gravity interpretation. This feature allows geophysicists to apply the method in areas where detailed geological information is limited (Reid and Allsop, 1990; Thompson, 1982). The expression for the three-dimensional Euler deconvolution is provided below:

$$N(B-G) = (x-x_0)\left(\frac{\partial G}{\partial x}\right) + (y-y_0)\left(\frac{\partial G}{\partial y}\right) + \\ +(z-z_0)\left(\frac{\partial G}{\partial z}\right) \quad (4)$$

In this context, G represents the gravitational field that is produced by the causative sources located at a specific point (x, y, z) in three-dimensional space. This point is referenced relative to the coordinates of the source (x_0, y_0, z_0). Additionally, the baseline level of the gravitational field is denoted as B, which serves as a reference value for the field's intensity. The structure index (N) is also incorporated, indicating the degree of homogeneity or the structural nature of the geological source, which can influence how the gravitational field is generated and observed.

- **2-D Modelling**

To achieve a more precise estimate of the anomaly depths, additional analysis is required. To better comprehend the basement's influence on the gravity data and to accurately map the basement rocks, a 2-D forward modelling technique was employed. The 2-D model for the study area was developed using the GM-SYS Geosoft program (Popowski et al., 2006), consisting of two primary layers: the basement and the overlying sediments. While a qualitative analysis of the gravity data can provide a general idea of the source parameters, a more in-depth approach is necessary for precise results. The initial density values used in the model were sourced from prior research, including studies by Talwani et al. (1959), Essed (1978), and Trepil et al. (2021). These density values were further refined using an apparent density filter, which calculates the apparent ground densities to

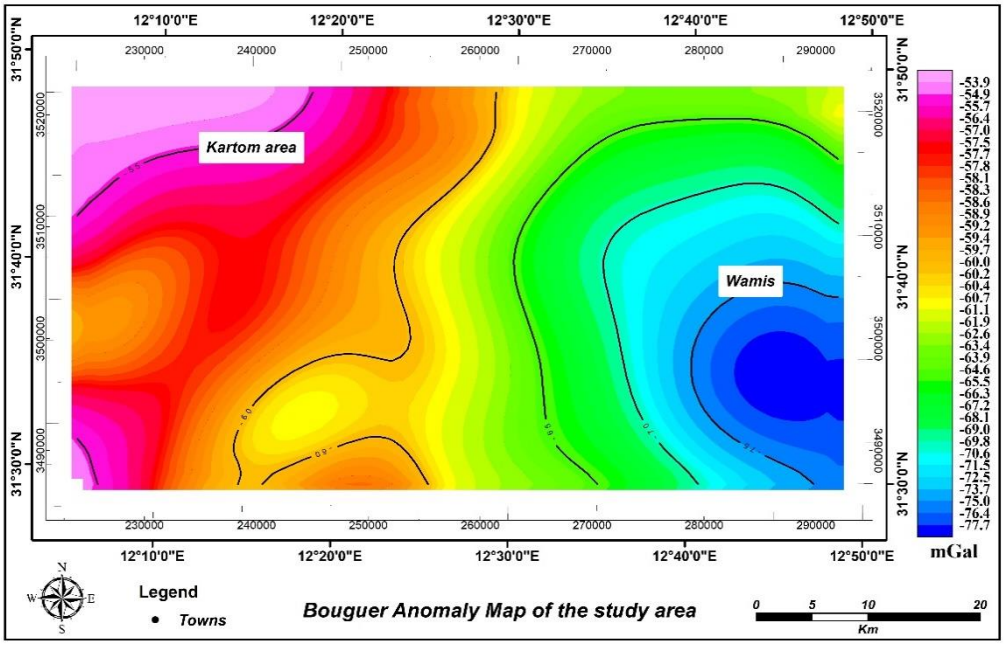

Fig. 2 Bouguer anomaly map of the study region.

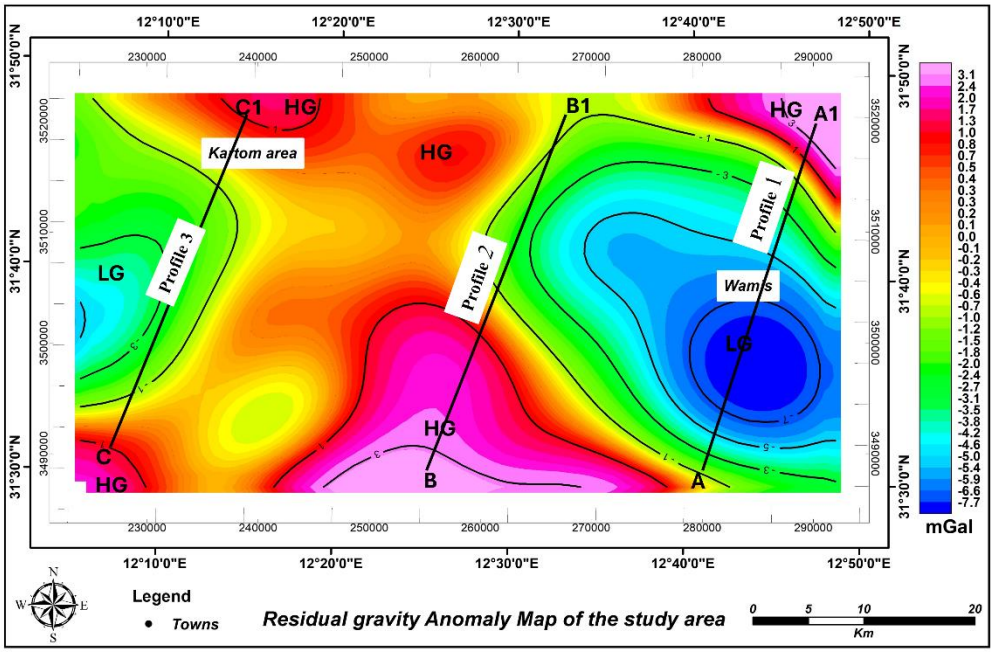

Fig. 3 Residual gravity anomaly map of the study region.

generate the observed gravity profile. The process was repeated multiple times to ensure the reliability of the results. The basement density was estimated at 2.67 g/cm³, based on gravity measurements taken from various elevations within the region.

RESULTS AND DISCUSSION

The Bouguer anomaly (BA) map for the study area is presented in Figure 2, displaying amplitude anomalies ranging from -77 mGal to -53 mGal. The residual gravity anomaly (RS) map (Fig. 3) shows amplitude anomalies within the study region ranging from -7.7 mGal to 3.1 mGal. This map primarily describes the major variations in the gravitational field of the shallow part of the crust, eliminates the regional ones, removes the effect of deeper structures, and describes the associated variations in its composition and sediment thickness. Four prominent gravity highs, located in the northeast (NE), southwest (SW), northwest (NW), and southern parts of the study area, are labelled HG. Additionally, two significant gravity lows in the eastern and western regions are labelled LG in the residual anomaly map. The anomaly signatures derived from gravity data suggest that edge

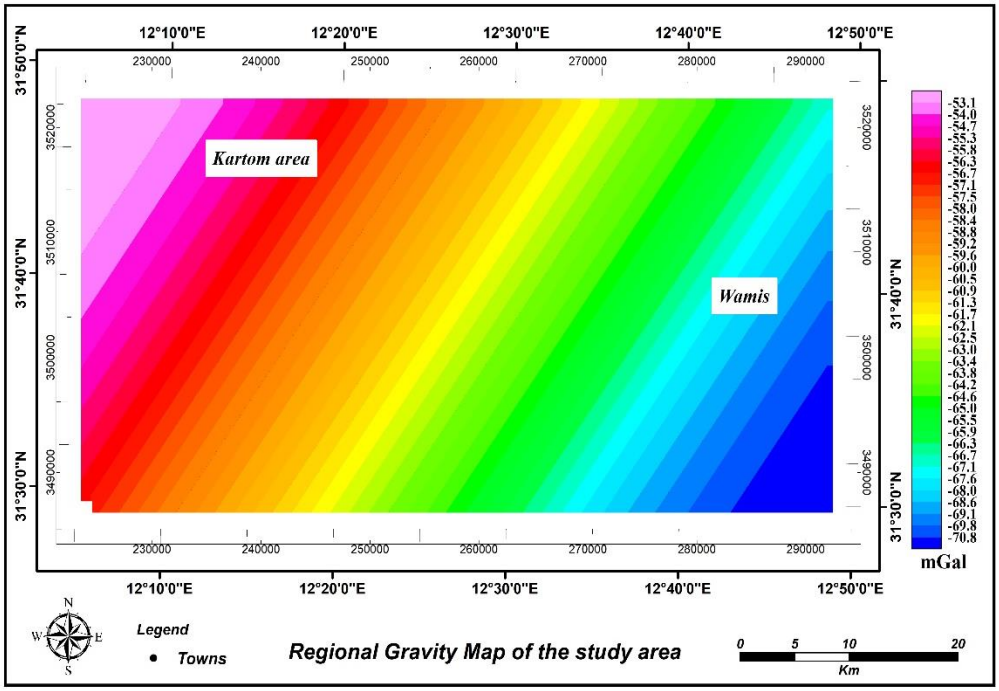

Fig. 4 Regional gravity map of the study region.

structures could correspond to geological contacts, faults, folds, or fractures. Furthermore, these anomalies are associated with variations in tectonic zones. The RS anomaly map reveals dominant anomaly trends in the NW-SE and NE-SW directions, which can be linked to various geological structures. Positive anomalies indicate regions with higher gravitational attraction, typically corresponding to areas of denser rock formations or deeper crustal structures. Conversely, lower gravity values are likely attributed to thick sedimentary deposits in different areas, which may represent sub-basins in the western and eastern parts of the study region. Negative anomalies indicate zones with weaker gravitational attraction, often associated with lower-density rock formations or shallower crustal structures.

The regional gravity anomaly map also shows high gravity values towards the northwest and low gravity values in the southeast. These are related to the existence of thick, high-density rocks at shallower depths in the northwest and low-density rocks in the southeast. Deeply buried structures were emphasised by regional gravity anomaly, as shown in Figure 4. The largest depression was mapped at the east part of the study area towards the southeast. This depression is consistent with the depressions mapped from the residual gravity anomaly. The existence of a large basin in the study area as represented by gravity lows demonstrates a possibility of high sediment accumulation, translating to hydrocarbon accumulation.

One of the most widely used techniques for delineating geological boundaries is the total horizontal gradient (THG) of the potential field, as proposed by Zhang et al. (2015). In this study, the total horizontal gradient was applied to the residual gravity anomaly (Fig. 5). The resulting map reveals strong horizontal gradient anomalies in the northeast (NE), southeast (SE), southwest (SW), and southern parts of the study area (marked as HG peaks). These anomalies delineate two major subsurface structural trends: NE-SW and NW-SE. These trends are attributed to various tectonic movements associated with a series of geological events, including the Hercynian tectonic activity, which disrupted the Mesozoic sedimentary sequence and led to the development of complex fault systems. However, it is important to note that potential field anomalies can exhibit high gravity values due to variations in rock density within the survey area. The dominant fault trend in the region is orientated in a northwest-southeast (NW-SE) direction, which is potentially related to the tectonic collision between the African and European plates that occurred during the Hercynian orogeny. Additionally, this fault trend may reflect the reactivation of older, upper Cretaceous lineaments within the Hun Graben. In contrast, the northeast-southwest (NE-SW) structural trend observed in the area is likely influenced by the well-established NNE-SSW structural features of Paleozoic rock formations, which are associated with the prominent Tibesti-Sirte Uplift. This structural framework suggests that the region's fault systems have been shaped by a combination of ancient and more recent tectonic processes, which include both collisional and reactivation events over geological time.

The Euler solution method proved to be highly effective in gravity interpretations due to its minimal requirement for prior knowledge about the source body's structure. The Euler deconvolution maps

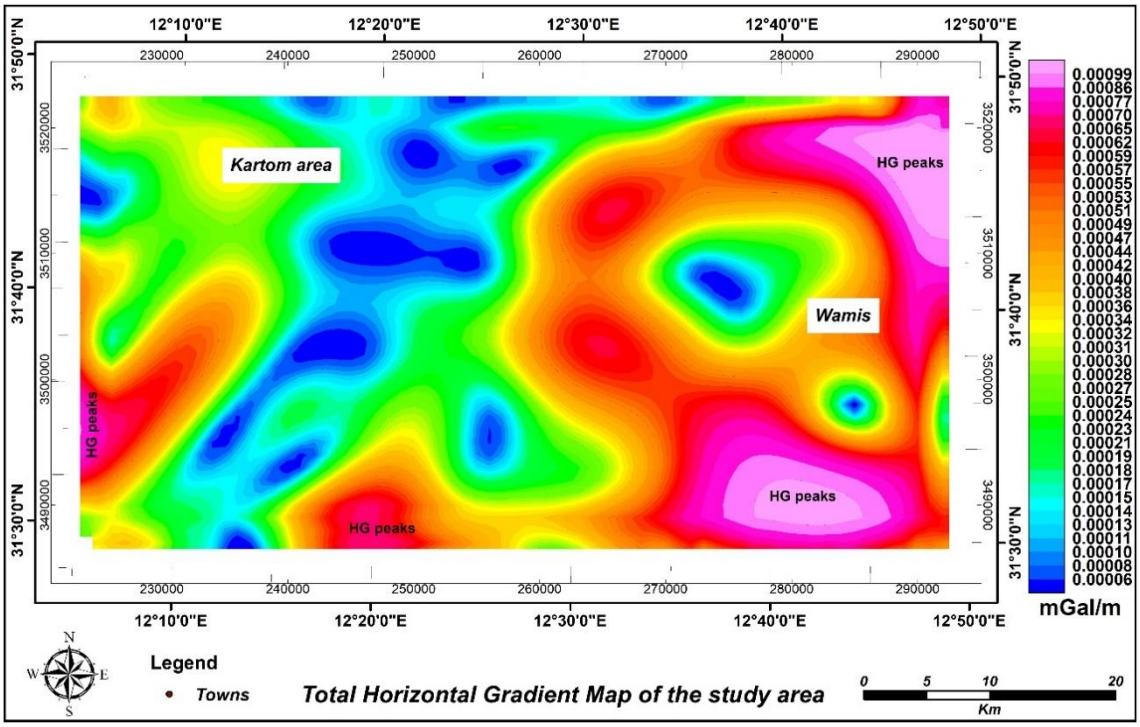

Fig. 5 Map resulting from applying the THG technique.

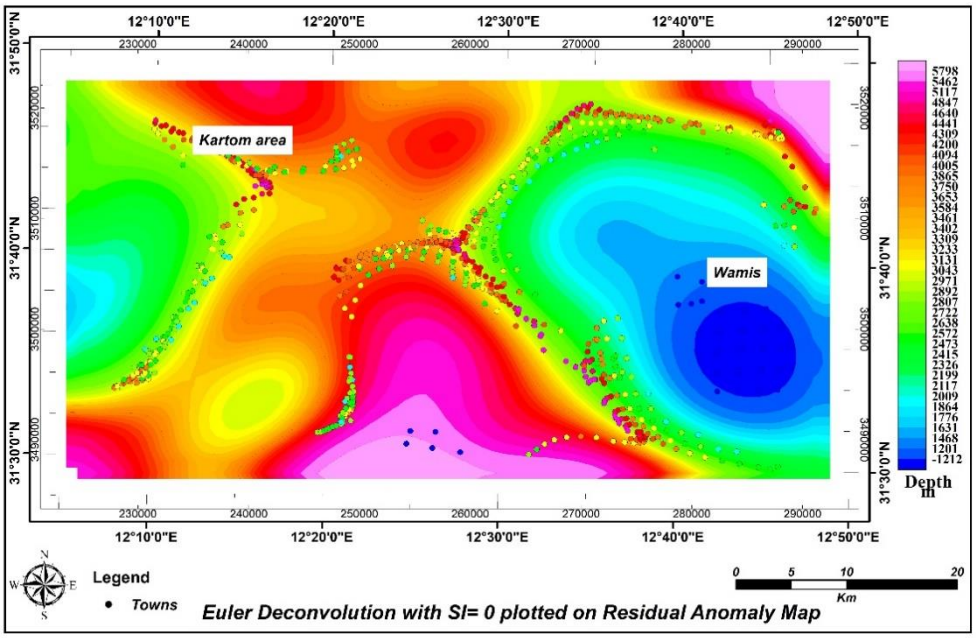

Fig. 6 3D Euler solutions map (W= 10, SI= 0).

(Fig. 6) were generated using a residual gravity map in Oasis Montaj based on standard Euler. A structural index of 0 was selected to identify the optimal solutions. The best clustering of source-depth solutions was achieved with a window size of 10x10 and a structural index of 0, allowing for a maximum depth tolerance of 15 %. This approach also superimposed major faults on the residual gravity map. The estimated depth of gravity sources ranged from 1200 m to 5798 m, with significant lineaments orientated NE-SW and NW-SE. These orientations likely correspond to the primary subsurface structures responsible for the gravity anomalies. Furthermore, most of the solutions are concentrated along the edges of the anomalies. Negative depth can correspond to topographic effects or surface density variations. The Euler solution map further corroborates the detection of trending faults, which were previously identified using the RS, THG, and TDR methods.

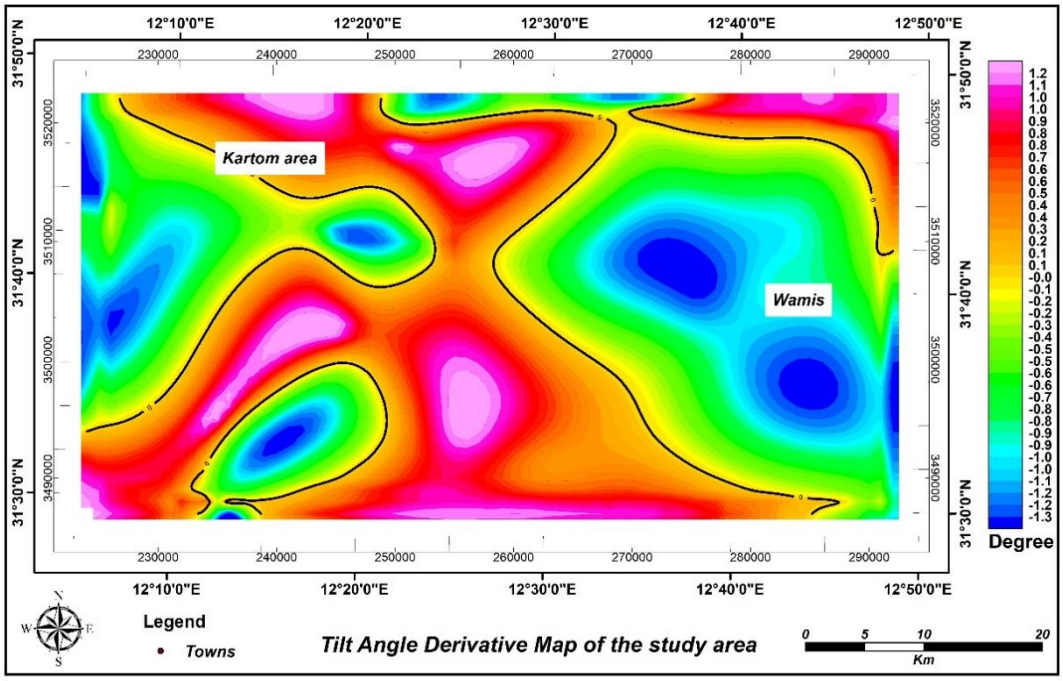

Fig. 7 Derivative of the tilt angle.

The zero value of the tilt angle marks the edges of the source body, making it a valuable tool for delineating boundaries. Positive tilt values are located directly above the sources, while negative values occur further away. The zero-contour lines on the tilt derivative anomaly map closely correspond with the peaks of the total horizontal gradient, aiding in the identification of major faults across different regions of the study area. Tilt derivative (TDR) filters often detect anomalies directly above their sources. The TDR analysis of gravity data (Fig. 7) highlights dominant fault trends with positive contrasts, primarily orientated in the northwest-southeast (NW-SE) and northeast-southwest (NE-SW) directions. The anomalies on the TDR map range in magnitude from -1.3 to 1.2 degrees. The results of this TDR analysis are consistent with previous studies conducted by Klitzsch (1970), Klitzsch and Gray (1971), and Desio et al. (1963), further confirming the structural trends and tectonic influences shaping the study region.

The primary structural map (Fig. 8) is developed by integrating key structural trends identified from the residual anomaly map, tilt derivative map, and Euler solution map derived from gravity data. This map provides a comprehensive representation of the geological framework within the study area, illustrating the distribution, orientation, and arrangement of faults and other structural features. The faults depicted in the map predominantly follow northwest-southeast (NW-SE) and northeast-southwest (NE-SW) orientations. These structural features reflect multiple tectonic episodes, including the formation of NE-SW lineaments during the early Paleozoic. The region's tectonic evolution is highly complex, beginning with the Late Precambrian Pan-African orogeny and extending through the Phanerozoic, characterised by the repeated reactivation of pre-existing structures. Lipparini (1968) suggested that the northwest-southeast fault displacement is associated with uplift events that occurred during the early Mesozoic. A key structural feature in the northern part of the study area is the Nafusah Uplift, which initially developed during the Hercynian orogeny but subsequently experienced subsidence, further influencing the region's geological evolution.

Gravity modelling of the residual field plays a crucial role in deciphering the region's complex geological structures, which are characterised by subsurface geological ambiguity and a higher basement density compared to the overlying sedimentary rocks. This density contrast makes gravity data a valuable tool for estimating basement depths (Blakely, 1995; Telford et al., 1990; Al-Heety and Eshwehdi, 2006; Schettino and Turco, 2011). In this study, geological and geophysical data were integrated to constrain subsurface structural models. Three gravity models were generated from the residual gravity data along profiles A-A1, B-B1, and C-C1. The 2-D profile models (Figs. 9 A, B, and C) were constructed along the NNE-SSW direction, each extending approximately 36 km. The estimated basement depth ranges from 1.2 to 3.53 km in profile 1, 1.8 to 2.7 km in profile 2, and 1.7 to 2.76 km in profile 3. The modelling results exhibit uncertainty errors of 0.714 % for profile 1, 0.093 % for profile 2, and 0.177 % for profile 3. The basement depth reaches approximately 2.8 km toward the east near the LG region, indicating a thick sedimentary cover. In contrast, sediment thickness gradually decreases in

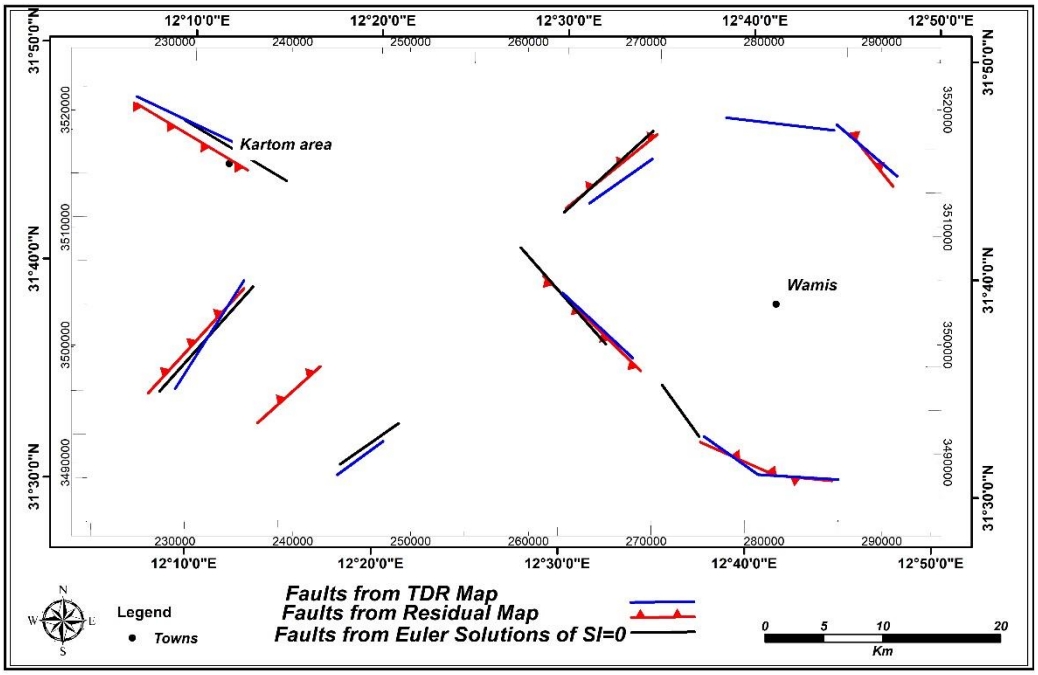

Fig. 8 Major faults map of the region from the residual map, TDR map, and Euler deconvolution.

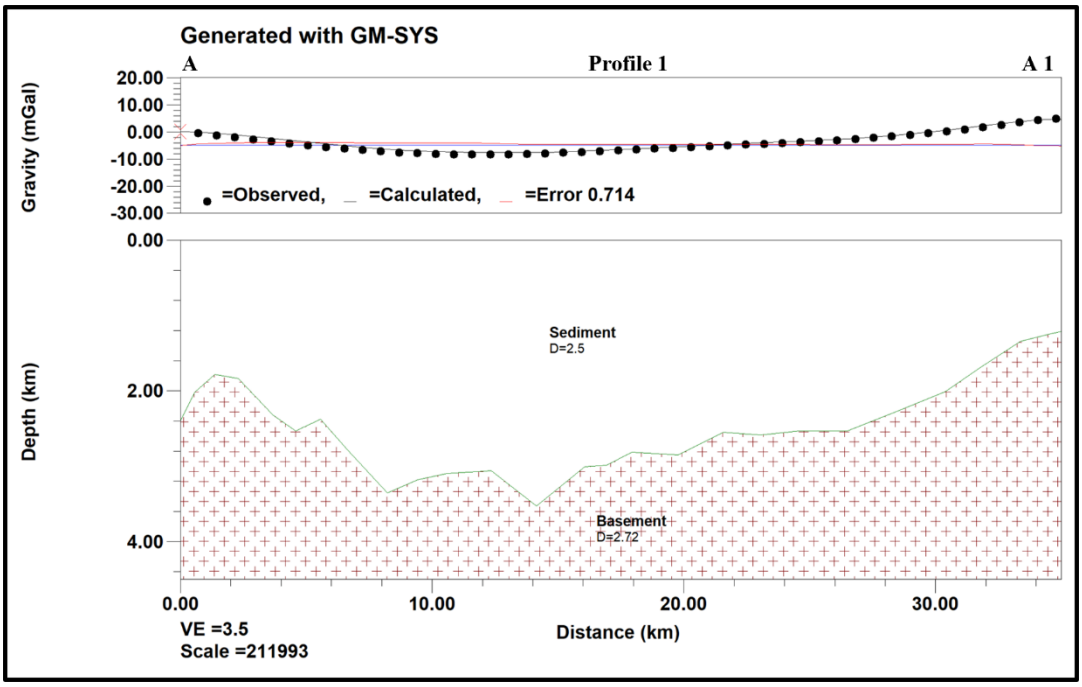

Fig. 9 (A) 2D forward modelling of Profile 1.

areas labelled HG. To validate the constructed models, the estimated basement depths were compared with previously reported values. According to Rusk (2001), Hallett (2002), and Saadi et al. (2009, 2011), the observed steep variations in the residual gravity anomaly suggest the presence of fault trends, which likely play a key role in shaping the subsurface structure. The basement surface appears to have been significantly influenced by tectonic processes, including subsidence in the eastern part of the study area due to the reactivation of the Pan-African fault system. During the Hercynian phase, the sub-basin experienced considerable uplift and erosion, resulting in the removal of a substantial portion of the Paleozoic sequence.

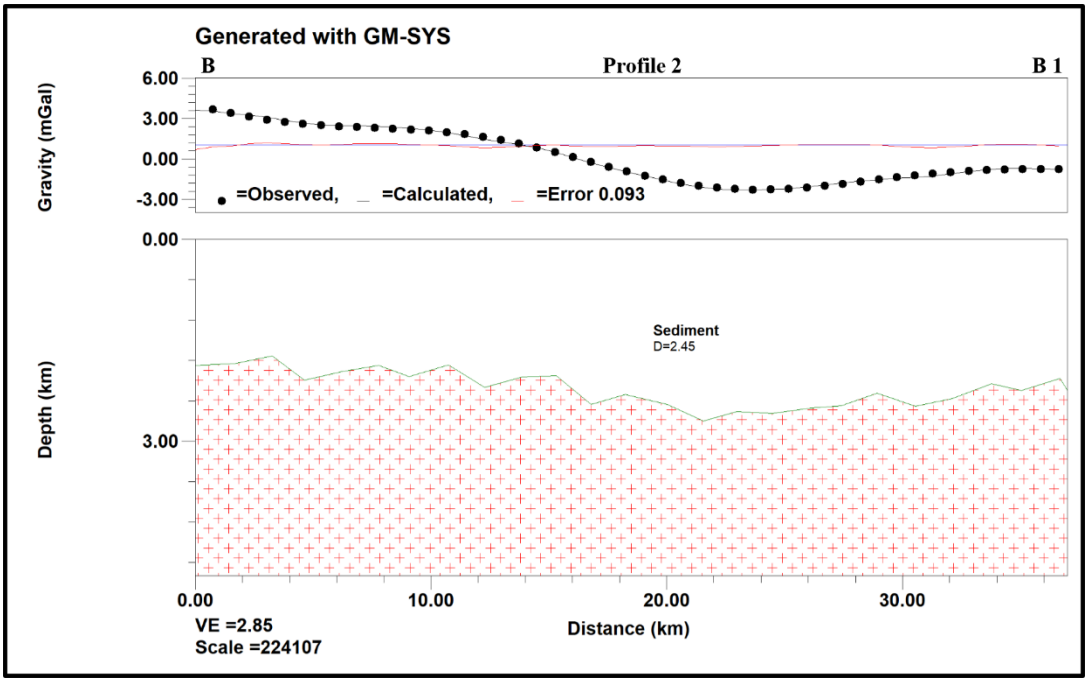

Fig. 9 (B) 2D forward modelling of Profile 2.

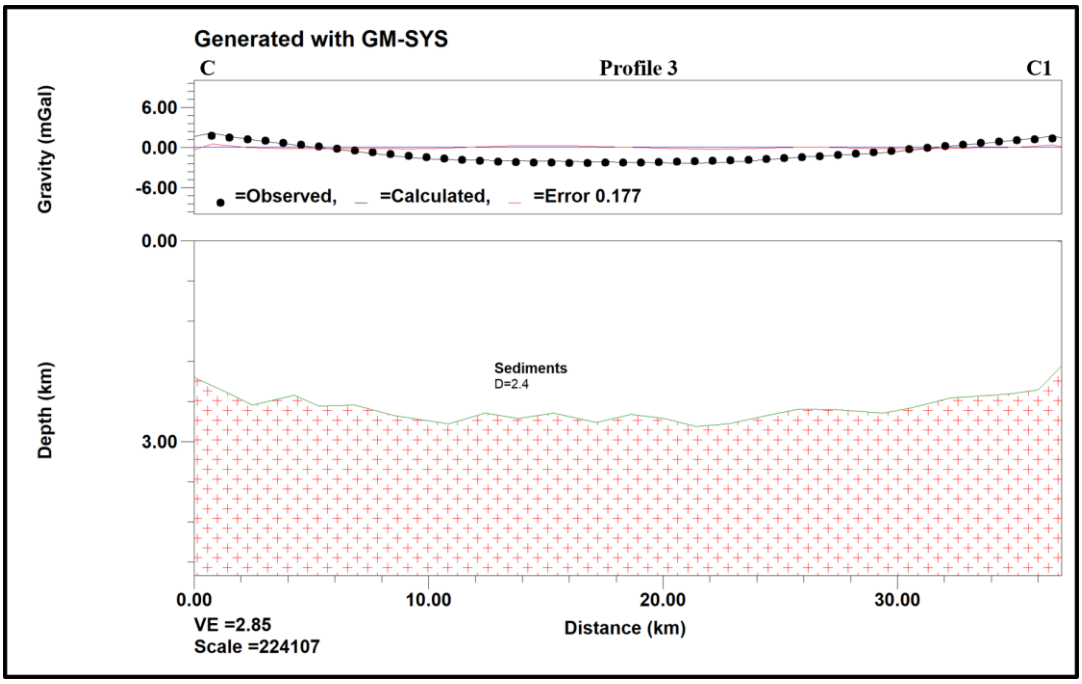

Fig. 9 (C) 2D forward modelling of Profile 3.

3. CONCLUSION

Despite more than 55 years of petroleum exploration in Libya, the geological structures of the region remain poorly understood. To address this, EIGEN-6C4 gravity data were analysed in the southern part of Jabal Nafusah, northwest Libya, to map subsurface structures and estimate basement rock depths. Several analytical methods, including high-pass filtering, total horizontal gradient, Euler solutions, and tilt derivative analysis, were applied to the gravity data to identify major structural faults. Additionally, 2-D forward modelling using GM-SYS within Oasis Montaj was conducted to estimate basement depths based on gravity data. The application of various filters to detect the edges of geological structures revealed dominant fault trends orientated in NW-SE and NE-SW directions, with source depths ranging from 1,200 to 5,798 m. The estimated basement depth varies across the profiles, ranging from 1.2 to 3.53 km in profile 1, 1.8 to 2.7 km in profile 2, and 1.7 to 2.76 km in profile 3. The basement depth reaches approximately 2.8 km toward

the east near the LG region, indicating a thick sedimentary cover. In contrast, sediment thickness gradually decreases in areas labelled HG. The structural map indicates that faults derived from the Euler solution align closely with those identified from residual anomalies and zero-contour lines of the tilt derivative map. These faults are linked to the tectonic evolution of the region, which began with Mesozoic basin extension during the Hercynian orogeny and is associated with the development of the North African platform in the early Paleozoic era.

ACKNOWLEDGEMENTS

Acknowledgement to the Ministry of Higher Education Malaysia for the Fundamental Research Grant Scheme with Project Code: FRGS/1/2022/STG08/USM/03/1 entitled "Performance-Based Multimodal Geophysical Design for Soil Dynamic Properties to Improve Visualisation of Subsurface Conditions" and also a research university grant entitled "Integrated Geophysical Characterisation of Geothermal Exploration and Strategy for the Sustainable Use of Geothermal Resources" with account no. 1001/PFIZIK/8011110.

REFERENCES

Abohajar, A., Krooss, B., Harouda, M. and Littke, R.: 2009, Maturity and source-rock potential of Mesozoic and Palaeozoic sediments, Jifarah Basin, NW Libya. J. Pet. Geol., 32, 4, 327–341. DOI: 10.1111/j.1747-5457.2009. 00453.x

Al-Heety, E.A. and Eshwehdi, A.: 2006, Seismicity of the northwestern region of Libya: an example of continental seismicity. Seismol. Res. Lett., 77, 6. 691–696. DOI: 10.1785/gssrl.77.6.691

Anketell, J.: 1996, Structural history of the Sirt Basin and its relationship to the Sabratah Basin and Cyrenaica Platform, northern Libya. In: Salem, M.J., Busrewil, M.T., Misallati, A.A. and Sola, M.A., Eds., The Geology of the Sirt Basin, III, Elsevier, Amsterdam, 57–89.

Araffa, S.A.S., Sabet, H.S. and Gaweish, W.R.: 2015, Integrated geophysical interpretation for delineating the structural elements and groundwater aquifers at central part of Sinai Peninsula, Egypt. J. Afr. Earth Sci., 105, 93–106.

Blakely, R.J.: 1995, Potential theory in gravity and magnetic applications. Cambridge University Press, Cambridge, 441 pp. DOI: 10.1017/CBO9780511549816

Burollet, P.F.: 1963, Saharan symposium, Field trip Guidebook of the Excursion to Jebel Nefusa. Petroleum Exploration Society of Libya, Tripoli.

Christie, A.M.: 1955, Geology of the Garian area. Tripolitania, Libya. U.N. Tech. Assistance Program Rept. TAA/LIB/2, 60 pp.

Christie, A.M.: 1966, Geology of the Garian Area, Tripolitania, Libya. Geological Section, Ministry of Industry. Bull. 5, 60 pp.

Cordell, L.: 1979, Gravimetric expression of graben faulting in Santa Fe Country and the Espanola Basin, New Mexico. Paper presented at the New Mexico Geological Society. Guidebook: 30th Field Conference, New Mexico, 59–64.

Darisma, D., Marwan, M. and Ismail, N.: 2019, Geological structure analysis of satellite gravity data in oil and gas prospect area of West Aceh-Indonesia. J. Aceh Phys. Soc., 8, 1, 1–5. DOI: 10.24815/jacps. v8i1.12750

Desio, A., Ronchetti, R.C., Pozzi, R., Clerici, F., Invernizzi, G., Pisoni, C. and Vigano, P.L.: 1963, Stratigraphic studies in the Tripolitanian Jebel (Libya). Riv. Ital. Paleontol. Stratigr., 9, 1–26.

Echikh, K.: 1998, Geology and hydrocarbon occurrences in the Ghadames basin, Algeria, Tunisia, Libya. Geol. Soc. Spec. Publ. London, 132, 1, 109–129.

Essed, A.S.: 1978, A reconnaissance Bouguer gravity map of Libya. M.Sc. Dissertation, Purdue University.

FitzGerald, D., Reid, A. and McInerney, P.: 2004, New discrimination techniques for Euler deconvolution. Paper presented at the 8th SAGA Biennial Technical Meeting and Exhibition. DOI: 10.1016/j.cageo.2004.03.006

Hallett, D.: 2002, Petroleum geology of Libya, 1st edition. Elsevier, Amsterdam, 503 pp.

Klitzsch, E.: 1970, The structural history of the Central Sahara: New insights into the structure and palaeogeography of a plateau. Geol. Rev., 59, 459–527.

Klitzsch, E. and Gray, C.: 1971, The structural development of parts of North Africa since Cambrian time. Paper presented at the Symposium on the geology of Libya. Tripoli, Faculty of Sciences, University of Libya, 256–260.

Kurniawan, F.A. and Aji, S.: 2012, Utilization of gravity anomaly data from GEOSAT and ERS-1 satellite images to model the geological structure of the Bentarsari Brebes basin. Indones. J. Appl. Phys., 2, 2, 1–14.

Lipparini, T.: 1968, Tectonics and geomorphology, Tripolitania area, Libya. Kingdom of Libya, Ministry of Industry.

Ma, G. and Li, L.: 2012, Edge detection in potential fields with the normalized total horizontal derivative. Comput. Geosci., 41, 83–87. DOI: 10.1016/j.cageo.2011.08.016

Mann, K.: 1975, Explanatory booklet, Sheet: Al Khums, NI 33-14. Geological map of Libya. Libyan Arab Republic, Industrial Research Centre Tripoli, 1–80.

Masoud, A.A. and Koike, K.: 2011, Auto-detection and integration of tectonically significant lineaments from SRTM DEM and remotely-sensed geophysical data. ISPRS J. Photogramm. Remote Sens., 66, 6, 818–832. DOI: 10.1016/j.isprsjprs.2011.08.003

Miller, H.G. and Singh, V.: 1994, Potential field tilt - a new concept for location of potential field sources. J. Appl. Geophys., 32, 2–3, 213–217. DOI: 10.1016/0926-9851(94)90022-1

Ming, Y., Ma, G., Li, L., Han, J. and Wang, T.: 2021, The spatial different order derivative method of gravity and magnetic anomalies for source distribution inversion. Remote Sens., 13, 5, 964. DOI: 10.3390/rs13050964

Pal, S.K. and Majumdar, T.: 2015, Geological appraisal over the Singhbhum-Orissa Craton, India using GOCE, EIGEN6-C2 and in situ gravity data. Int. J. Appl. Earth Obs. Geoinf., 35, 96–119. DOI: 10.1016/j.jag.2014.06.007

Pal, S., Narayan, S., Majumdar, T. and Kumar, U.: 2016 Structural mapping over the 85 E Ridge and surroundings using EIGEN6C4 high-resolution global combined gravity field model: an integrated approach. Mar. Geophys. Res., 37, 3, 159–184. DOI: 10.1007/s11001-016-9274-3

Northwest Geophysical Associates Inc.: 2004, GM-SYS gravity/magnetic modeling software: User's guide.

Reid, A. and Allsop, J.G.H., Millet, A. and Somerton, I.: 1990, Magnetic interpretation in three dimensions using Euler Deconvolution. Geophysics, 55, 80–91. DOI: 10.1190/1.1442774

Rusk, D.C.: 2001, Libya: Petroleum potential of the underexplored basin centers – A twenty-first-century challenge. AAPG Memoir, 74, 429–452.

Saadi, N.M., Aboud, E. and Watanabe, K.: 2009, Integration of DEM, ETM+, geologic, and magnetic data for geological investigations in the Jifara Plain, Libya. IEEE Trans. Geosci. Remote Sens., 47, 10, 3389–3398. DOI: 10.1109/TGRS.2009.2020911

Saadi, N.M., Zaher, M.A., El-Baz, F. and Watanabe, K.: 2011, Integrated remote sensing data utilization for investigating structural and tectonic history of the Ghadames Basin, Libya. Int. J. Appl. Earth Obs. Geoinf., 13, 5, 778–791. DOI: 10.1016/j.jag.2011.05.016

Sadeghi, B., Khalajmasoumi, M., Afzal, P., Moarefvand, P., Yasrebi, A.B., Wetherelt, A. and Ziazarifi, A.: 2013, Using ETM+ and ASTER sensors to identify iron occurrences in the Esfordi 1: 100,000 mapping sheet of Central Iran. J. Afr. Earth Sci., 85, 103–114. DOI: 10.1016/j.jafrearsci.2013.05.003

Salehi, R., Saadi, N.M., Khalil, A. and Watanabe, K.: 2015, Integrating remote sensing and magnetic data for structural geology investigation in pegmatite areas in eastern Afghanistan. J. Appl. Remote Sens., 9, 1, 096097. DOI: 10.1117/1.JRS.9.096097

Schettino, A. and Turco, E.: 2011, Tectonic history of the western Tethys since the Late Triassic. Geol. Soc. Am. Bull., 123, 1-2, 89–105. DOI: 10.1130/B30064.1

Steckler, M.S., Berthelot, F., Lyberis, N. and Le Pichon, X.: 1988, Subsidence in the Gulf of Suez: implications for rifting and plate kinematics. Tectonophysics, 153, 1-4, 249–270. DOI: 10.1016/0040-1951(88)90019-4

Subba Rao, D.V.: 1996, Resolving Bouguer anomalies in continents-a new approach. Geophys. Res. Lett., 23, 24, 3543–3546. DOI: 10.1029/96GL03471

Swire, P. and Gashgesh, T.: 2000, The Bio–Chrono—and Lithostratigraphy and hydrocarbon productivity of the NW Ghadamis Basin and Jifarah Plain. In: Salem, M.J. and Khaled, M.O., (Eds., The geology of Northwest Libya. Gutenberg Press, Malta, 1, 173–216.

Talwani, M., Worzel, J.L. and Landisman, M.: 1959, Rapid gravity computations for two-dimensional bodies with application to the Mendocino submarine fracture zone. J. Geophys. Res., 64, 1, 49–59. DOI: 10.1029/JZ064i001p00049

Tedla, G.E., Van Der Meijde, M., Nyblade, A. and Van der Meer, F.: 2011, A crustal thickness map of Africa derived from a global gravity field model using Euler deconvolution. Geophys. J. Int., 187, 1, 1–9. DOI: 10.1111/j.1365-246X.2011.05140.x

Telford, W.M., Geldart, L. P. and Sheriff, R. E.: 1990, Applied Geophysics. Cambridge University Press.

Thompson, D.: 1982, EULDPH: A new technique for making depth estimates from magnetic data computer assisted depth estimates from magnetic data. Geophysics, 47, 31–37. DOI: 10.1190/1.1441278

Trepil, F., Kahoul, S., Uyimwen, O.A., Eshanibli, A., Ismail, N.A., and Ghanoush, H.: 2021, Delineation of structure elements and the basement depth at the Jifara Plain NW Libya using integration application of potential field dataset. Acta Geodyn. Geomater., 18, 1, 83–90. DOI: 10.13168/AGG.2021.0006

Trepil, F., Muztaza, N.M., Abir, I.A., Saleem, M.A., Khalf, K.A. and Sharoni, S.M.: 2024, Identifying the geological structure of the Garyan area in Northwest Libya using EIGEN-6C4 satellite gravity data. Acta Geodyn. Geomater., 21, 2, 111–120. DOI: 10.13168/AGG.2024.0010

Trepil, F., Muztaza, N.M., Abir, I.A., Saleem, M.A., Zulaikah, S. and Teoh Ying, J.I.A.: 2023, Delineating structure elements and depth of sources using an aeromagnetic dataset in the Tarhona region, Northwest Libya. Acta Geodyn. Geomater., 20, 3. DOI: 10.13168/AGG.2023.0008

Van de Weerd, A.A. and Ware, P.L.G.: 1994, A review of the East Algerian Sahara oil and gas province (Triassic, Ghadames and Illizi basins). First Break, 12, 7. DOI: 10.3997/1365-2397.1994023

Zeinelabbdein, K.A., Elmam, M.S., Ali, H.A. and Alhassan, O.M.: 2014, An integrated analysis of landsat OLI image and satellite gravity data for geological mapping in North Kordofan State, Sudan. J. South Am. Earth Sci., 1, 11, 25–32.

Zhang, X., Yu, P. Tang, R. Xiang, Y. and Zhao, C.J.: 2015, Edge enhancement of potential field data using an enhanced tilt angle. Explor. Geophys., 46, 3, 276–283. DOI: 10.1071/EG13104